

Advanced continuous wavelet transform algorithm for digital interferogram analysis and processing

Zhaoyang Wang

The Catholic University of America
Department of Mechanical Engineering
Washington, DC 20064
E-mail: wangz@cua.edu

Huanfeng Ma

University of Maryland
Department of Electrical and Computer
Engineering
College Park, Maryland 20742

Abstract. An advanced continuous wavelet transform algorithm for digital interferogram analysis and processing is proposed. The algorithm is an extension of the traditional wavelet transform; the mother wavelet and normalization parameter are selected based on the characteristics of optical interferograms. To reduce the processing time, a fast Fourier transform scheme is employed to implement the wavelet transform calculation. The algorithm is simple and is a robust tool for interferogram filtering and for whole-field fringe and phase information detection. The concept is verified by computer simulation and actual experimental interferogram analysis. © 2006 Society of Photo-Optical Instrumentation Engineers. [DOI: 10.1117/1.2188399]

Subject terms: wavelet transform; interferogram analysis; interferogram processing.

Paper 050299R received Apr. 19, 2005; revised manuscript received Aug. 18, 2005; accepted for publication Aug. 29, 2005; published online Apr. 3, 2006.

1 Introduction

Among the numerous computer-aided digital interferogram-processing algorithms capable of extracting whole-field information on phase distributions (or fractional fringe orders) from one or more interferograms, the most predominantly used ones are those that can automatically analyze interferograms. Typical automatic phase analysis methods include the phase-shifting method, the Fourier transform method, and the wavelet transform method. Compared with the phase-shifting method, where a series of phase-shifted interferograms are required, the Fourier transform and wavelet transform methods have the capability to extract phase information from one single interferogram.

In the Fourier transform method, the first harmonic of the Fourier spectra of an interferogram in the frequency domain is extracted and inversely transformed to obtain the whole-field phase distributions. This is a simple and fast procedure; however, an accurate extraction of the first harmonic is impractical in real applications. The reason for this is that the Fourier transform yields the spectra of the entire interferogram and the spectra do not accurately reflect the local fringe information.

In recent years, the wavelet transform has been successfully applied to image and signal processing.¹ Unlike the Fourier transform, the wavelet transform can detect the characteristics of local signals. Therefore, the wavelet transform is particularly helpful for the analysis and processing of interferograms where local fringe information is important. Research on the wavelet transform for interferogram processing has been active for a decade, and different schemes have been proposed. Early work includes the applications of a one-dimensional (1-D) wavelet transform to

the phase analysis of the grid method by Morimoto and Imamoto² and to the white-light interferometry by Sandoz.³ Tomassini et al.⁴ proposed a 1-D wavelet transform ridge extraction technique for interferogram analysis. Recently, Liu et al.^{5,6} proposed 1-D wavelet transform methods for phase extraction in moiré interferometry; Zhong and Weng⁷ proposed a 1-D wavelet transform profilometry for carrier-fringe pattern analysis. The methods cited utilize 1-D wavelet transforms for interferogram processing; their accuracies are limited due to the simplification of 2-D interferograms to 1-D transformations. To analyze moiré interferograms in 2-D, Kadooka et al.⁸ proposed an algorithm using a 2-D continuous wavelet transform to improve processing accuracies. However, their algorithm is very complicated and is only suitable for interferograms with sufficiently uniform fringes. It should be noted that all these methods require long computation times, and none of them have yielded examples with analysis results that are comparable with the ones obtained using other widely used processing techniques such as the phase-shifting method.

In this paper a novel, advanced 2-D continuous wavelet transform algorithm capable of handling the mentioned problems in the existing methods is proposed. The algorithm is simple and fast; it is effective for general interferogram processing such as interferogram filtering and phase extractions. The details of the proposed algorithm are described below.

2 Advanced 2-D Continuous Wavelet Transform Algorithm

The intensity of an interferogram can be expressed as

$$I(\mathbf{x}) = I_0(\mathbf{x}) + I_a(\mathbf{x}) \cos \phi(\mathbf{x}), \quad (1)$$

where $\mathbf{x}=(x,y)$ comprises the 2-D coordinates of the individual pixel in the interferogram, $I_0(\mathbf{x})$ is the background or

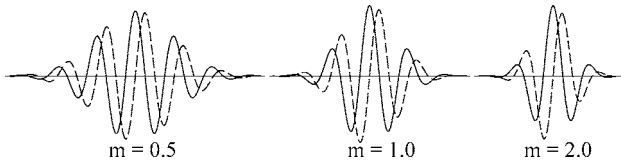


Fig. 1 Modified Morlet wavelet with different m .

mean intensity, $I_a(\mathbf{x})$ is the modulation amplitude, and $\phi(\mathbf{x})$ is the angular phase information.

In this proposed algorithm, the wavelet transform of an interferogram $I(\mathbf{x})$ is defined as

$$W(\mathbf{b}, a, \theta) = a^{-n} \int_{-\infty}^{\infty} I(\mathbf{x}) \cdot \psi^*[a^{-1} \mathbf{r}_{-\theta}(\mathbf{x} - \mathbf{b})] d^2\mathbf{x}, \quad (2)$$

where $a > 0$ is a scale dilation parameter corresponding to the width of the wavelet, \mathbf{b} is a 2-D translation parameter corresponding to the position of the wavelet, θ is a rotation parameter, $\mathbf{r}_{-\theta}$ is the conventional 2×2 rotation operator matrix, $\psi(\mathbf{x})$ is the mother wavelet, ψ^* denotes the complex conjugate of ψ , n is the normalization parameter, and $W(\mathbf{b}, a, \theta)$ is the wavelet transform coefficient.

In general signal and image processing using wavelet transforms, one typical mother wavelet employed to detect oriented features is the Morlet wavelet. In the proposed algorithm, the 2-D Morlet wavelet is chosen and modified for interferogram processing. The modified wavelet is expressed as

$$\psi(\mathbf{x}) = \exp(-m|\mathbf{x}|^2 + i2\pi x), \quad (3)$$

where m is a parameter to be determined as described below.

The basic principle of wavelet transform analysis is to find a certain scale parameter a and rotation parameter θ that make the mother wavelet best match the local signal. For interferograms composed of fringes, it is well known that the ideal way to analyze fringes is using local gratings with proper frequencies and orientations to match the local interferogram fringes. This is the reason the wavelet transform is suitable for interferogram processing. To find the proper parameter m for the mother wavelet, the corresponding real parts (solid lines) and imaginary parts (dashed lines) of the 1-D mother wavelet function with $m=0.5$, 1.0, and 2.0 are illustrated in Fig. 1. Since the fringe frequencies and orientations may have large variations across an interferogram, the ideal width of the mother wavelet should be about one period. Consequently, $m=2.0$ is a better selection than $m=0.5$, though the latter yields the traditional Morlet wavelet function and has been employed in existing algorithms.²⁻⁸ The superiority of $m=2.0$ to $m=0.5$ has been demonstrated by a number of different experimental interferograms, regardless of the actual level of noise in them.⁹ An accurate determination of the best m is related to the actual interferograms and the Gaussian distribution of the wavelet function. A future study will focus on optimizing m . In this proposed algorithm, m is set to 2.0.

Denoting the local fringe period, orientation, and angular phase at an arbitrary point \mathbf{b} in an interferogram as A ($A > 0$), Θ , and Φ , respectively, the local interferogram can be theoretically expressed as

$$I'(\mathbf{x}) = I_0 + I_a \left[2\pi \frac{(x - b_x) \cos \Theta + (y - b_y) \sin \Theta}{A} + \Phi \right]. \quad (4)$$

It should be noted that I_0 and I_a are assumed to be constants in the local region around point \mathbf{b} . The corresponding wavelet transform of the theoretical local interferogram is

$$W'(\mathbf{b}, a, \theta) = a^{-n} \int_{-\infty}^{\infty} I'(\mathbf{x}) \cdot \psi^*[a^{-1} \mathbf{r}_{-\theta}(\mathbf{x} - \mathbf{b})] d^2\mathbf{x}. \quad (5)$$

The Gaussian distribution of the wavelet function at point \mathbf{b} ensures

$$W'(\mathbf{b}, a, \theta) = W(\mathbf{b}, a, \theta), \quad (6)$$

where $W(\mathbf{b}, a, \theta)$ and $W'(\mathbf{b}, a, \theta)$ are governed by Eq. (2) and (5), respectively.

Substituting Eqs. (3) and (4) into Eq. (5) involves a simple but tedious procedure. For simplicity, only the final result is listed below:

$$W'(\mathbf{b}, a, \theta) = a^{2-n} \left[I_0 \frac{\pi}{m} \exp\left(-\frac{\pi^2}{m}\right) + \frac{I_a \pi}{2m} \exp\left(-\frac{\pi^2}{m} \left\{ \left(\frac{a}{A} - 1\right)^2 + 2\frac{a}{A} [1 - \cos(\Theta - \theta)] \right\}\right) \exp(i\Phi) + \frac{I_a \pi}{2m} \exp\left(-\frac{\pi^2}{m} \left\{ \left(\frac{a}{A} + 1\right)^2 - 2\frac{a}{A} [1 - \cos(\Theta - \theta)] \right\}\right) \exp(-i\Phi) \right]. \quad (7)$$

Equation (7) clearly shows that n should be set to 2 to normalize the wavelet transform coefficients. It is noteworthy that this selection of n is different from the one employed in conventional image and signal processing, where n is set to 0.5 and 1 for 1-D and 2-D cases, respectively.¹ Setting n to 1 for 1-D optical signal analysis was initially proposed by Telfer and Szu,¹⁰ and the proposal was then directly adopted in later work such as Refs. 2, 5, and 8. Our proposed approach for the first time, to the best of our knowledge, theoretically and strictly verifies the correct determination of n .

Now, with the normalization parameter $n=2$, it is evident that the wavelet transform coefficient with maximum magnitude can be obtained when $a=A$ and $\theta=\Theta$. In this case, the third term in Eq. (7) can be neglected, since it is much smaller than the second term. Consequently, Eq. (7) can be simplified as

$$W^*(\mathbf{b}, a, \theta) = I_0 \frac{\pi}{m} \exp\left(-\frac{\pi^2}{m}\right) + \frac{I_a \pi}{2m} \exp(i\Phi). \quad (8)$$

From Eq. (6) and Eq. (8), the phase at point \mathbf{b} can be calculated from

$$\phi(\mathbf{b}) = \Phi = \tan^{-1}\left(\frac{\text{Im } W(\mathbf{b}, a, \theta)}{\text{Re } W(\mathbf{b}, a, \theta) - I_0(\pi/m) \exp(-\pi^2/m)}\right), \quad (9)$$

where Im and Re denote the imaginary and real parts of a complex value, respectively, and I_0 can be set equal to the mean intensity of the interferogram.

Equation (9) shows that it is theoretically quite simple to extract phase distributions from interferograms. In practice, however, a direct numerical calculation of Eq. (2) is extremely time-consuming. This is another serious limitation of the existing 1-D and 2-D algorithms.²⁻⁸ Actually, there is a well-known procedure in signal processing that can be employed to reduce the computation time of a wavelet transform, and the algorithm is introduced below.

Defining $\mathbf{T}=(T_x, T_y)=a^{-1}\mathbf{r}_-\theta(\mathbf{x}-\mathbf{b})$, then

$$\begin{aligned} T_x &= a^{-1}[(x-b_x)\cos\theta + (y-b_y)\sin\theta], \\ T_y &= a^{-1}[-(x-b_x)\sin\theta + (y-b_y)\cos\theta]. \end{aligned} \quad (10)$$

From Eq. (3), we get

$$\psi(\mathbf{T}) = \exp(-m|\mathbf{T}|^2 + i2\pi T_x). \quad (11)$$

Therefore,

$$\begin{aligned} \psi^*(\mathbf{T}) &= \exp(-m|\mathbf{T}|^2 + i2\pi T_x) \\ &= \exp\{-ma^{-2}[(x-b_x)^2 + (y-b_y)^2] \\ &\quad + i2\pi a^{-1}[(b_x-x)\cos\theta + (b_y-y)\sin\theta]\} \\ &= \zeta(\mathbf{b}-\mathbf{x}), \end{aligned} \quad (12)$$

where

$$\zeta(\mathbf{x}) = \exp[-ma^{-2}(x^2 + y^2) + i2\pi a^{-1}(x\cos\theta + y\sin\theta)]. \quad (13)$$

With Eqs. (10) and (12), Eq. (2) can be simplified as

$$\begin{aligned} W(\mathbf{b}, a, \theta) &= a^{-n} \int_{-\infty}^{\infty} I(\mathbf{x}) \cdot \psi^*(\mathbf{T}) d^2\mathbf{x} \\ &= a^{-n} \int_{-\infty}^{\infty} I(\mathbf{x}) \cdot \zeta(\mathbf{b}-\mathbf{x}) d^2\mathbf{x}. \end{aligned} \quad (14)$$

Equation (14) involves a convolution of two functions. The time-consuming convolution operation can be implemented using the fast Fourier transforms (FFT) described as follows:

$$\begin{aligned} W(\mathbf{b}, a, \theta) &= a^{-n} \int_{-\infty}^{\infty} I(\mathbf{x}) \cdot \zeta(\mathbf{b}-\mathbf{x}) d^2\mathbf{x} = a^{-n} I(\mathbf{x}) * \zeta(\mathbf{x}) \\ &= a^{-n} F^{-1}\{F[I(\mathbf{x})] \cdot F[\zeta(\mathbf{x})]\}, \end{aligned} \quad (15)$$

where * denotes convolution and \cdot denotes ordinary multi-

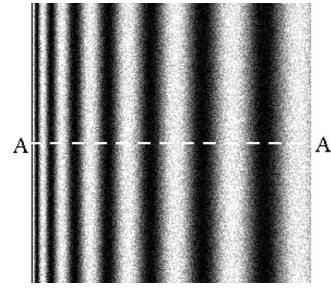


Fig. 2 Computer-generated phase map with random noise ranging from $-\pi/4$ to $\pi/4$.

plication, and where F and F^{-1} denote the forward and inverse fast Fourier transforms, respectively.

The wavelet transform based on the fast algorithm can significantly reduce the computation time. With a total pixel number of N , a direct numerical calculation of Eq. (2) requires on the order of N^2 operations, while FFT-based fast calculation requires on the order of $N \log_2 N$ operations. This indicates that the fast calculation is at least a few thousands times faster than a direct calculation for a typical interferogram larger than 128 by 128 pixels; the efficiency will be even higher if the image is larger.

The proposed algorithm can be summarized as follows: for any arbitrary pair a and θ , the wavelet transform coefficients at all points in the interferogram can be calculated by using Eq. (15). The pair (a, θ) that yield the maximum wavelet transform coefficient at each point denote the local fringe period (frequency is $1/a$) and orientation at the same point, and the phase can be calculated from Eq. (9). It should be noted that there is no available theoretical guidance on determining the sampling intervals of the parameters a and θ . In practice, a trade-off between finer parameter intervals and shorter computation times needs to be considered.

Once the phase information, fringe frequency, and orientation are obtained, they can be directly employed for further interferogram analysis and processing, such as determination of fringe order gradients, by

$$\begin{aligned} g_x &= a^{-1} \cos \theta, \\ g_y &= a^{-1} \sin \theta. \end{aligned} \quad (16)$$

The phase distributions can also be utilized to filter interferograms through reconstructing fringes. For a 255-graylevel interferogram, the filtered interferogram can be obtained, after normalizing background intensities and modulation amplitudes, from

$$I'(\mathbf{x}) = 127.5[1 + \cos \phi(\mathbf{x})]. \quad (17)$$

3 Simulation and Experiment

A computer simulation was conducted to verify the concept. The interferogram used in the simulation is shown in Fig. 2, which represents a monotonically increasing phase map with random noise from $-\pi/4$ to $\pi/4$. Figure 3 shows the real phase gradients and the ones detected by using the proposed algorithm, Kadooka's algorithm,⁸ and Liu's algorithm⁶ along the horizontal center line AA' in the inter-

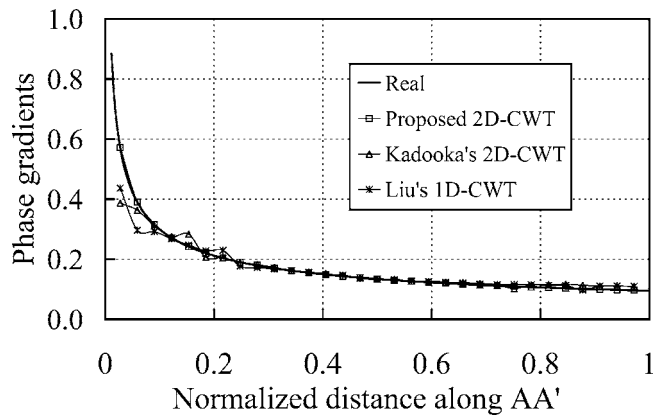


Fig. 3 Phase gradients along the horizontal centerline AA'.

ferogram of Fig. 2. With the simple but typical simulated interferogram, the simulation clearly indicates that the proposed algorithm provides superior results for phase extractions.

The proposed algorithm was then applied to the real interferogram in Fig. 4(a), which represents the thermally induced vertical displacement fringe pattern of a solder ball interconnection in an electronic packaging component; the

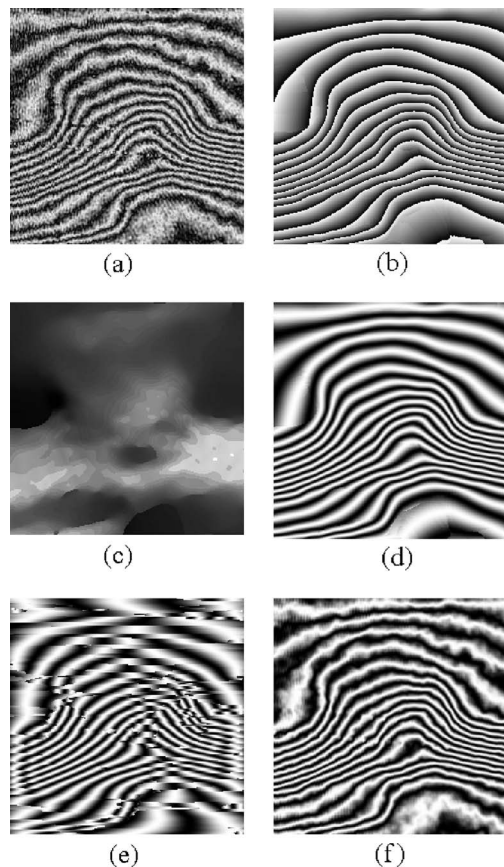


Fig. 4 Application of the proposed wavelet transform algorithm: (a) initial interferogram, (b) wrapped phase map, (c) map of fringe order gradients, (d) reconstructed interferogram, (e) reconstructed interferogram using 1-D wavelet transform algorithm, (f) reconstructed interferogram using spatial filtering and phase-shifting technique.

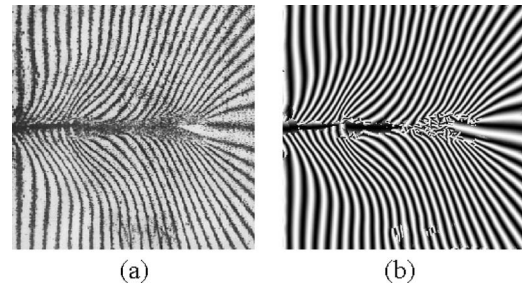


Fig. 5 Example of one limitation of the proposed wavelet transform algorithm: (a) initial interferogram with geometric discontinuities and erroneous breaks, (b) reconstructed interferogram with apparent errors located in areas of boundaries, discontinuities, and breaks.

experiment was implemented by using microscopic moiré interferometry. Figure 4(b)–4(d) show the results, where (b) is the wrapped phase map, (c) is the map of fringe order gradients, and (d) is the reconstructed interferogram. As comparisons, Figs. 4(e) and 4(f) show the reconstructed interferograms obtained by using the 1-D wavelet transform algorithm and the phase-shifting technique (combined with spatial filtering), respectively. It is evident that the proposed algorithm yields results that are qualitatively better defined. The experiment proved the validation of the proposed algorithm.

4 Discussion

Applications to computer simulations and actual experiments show that the proposed wavelet transform algorithm is a very powerful tool for interferogram analysis even when there exist high-level noises in the images. In spite of its apparent advantages, however, the proposed algorithm also has limitations in real applications.

It is understood from Eq. (2) that the continuous wavelet transform requires the intensity function $I(\mathbf{x})$ be an infinite continuous function. In reality, an interferogram image always has boundaries and there might also be material or geometric discontinuities and erroneous breaks in the interferogram. Consequently, the data located very close to the image boundaries, discontinuities, and breaks generally cannot be accurately analyzed. This is one limitation of the proposed method. Figure 5 shows one example where the initial moiré interferometry pattern contains geometric discontinuities (i.e., a crack) in the center region and erroneous breaks in the lower area. The corresponding errors in the reconstructed interferogram are evident.

Unlike the phase-shifting algorithm, which uses a series of phase-shifted interferograms so that directions of phase gradients can be obtained, the algorithms based on a single interferogram, including the proposed algorithm, cannot provide information on the directions of phase gradients. In other words, the single-interferogram-based algorithms provide absolute phase gradients only and cannot distinguish between positive and negative gradients. This could be a major disadvantage, for fully automatic analyses of complex interferograms (e.g., enclosed circular fringes), of all such algorithms, including the proposed one.

5 Conclusion

In conclusion, an algorithm that uses an advanced 2-D continuous wavelet transform to extract whole-field fringe and phase information from interferograms is proposed. The wavelet transform parameters employed in the new algorithm are appropriately determined based on the local fringe characteristics. To reduce the processing time, a fast Fourier transform scheme is employed, and it makes the proposed wavelet transform technique practical for actual applications. The algorithm is simple and fast, and simulation and experimental results proved its effectiveness.

References

1. J. Antoine, "The continuous wavelet transform in image processing," *CWI Q.* **11**(4), 323–345 (1998).
2. Y. Morimoto and Y. Imamoto, "Application of wavelet transform to displacement and strain measurement by grid method," in *Proc. SEM Spring Conference on Experimental Mechanics*, pp. 898–903, Society for Experimental Mechanics, Bethel (1995).
3. P. Sandoz, "Wavelet transform as a processing tool in white-light interferometry," *Opt. Lett.* **22**(14), 1065–1067 (1997).
4. P. Tomassini, A. Giulietti, L. Gizzi, M. Galimberti, D. Giulietti, N. Borghesi, and O. Willi, "Analyzing laser plasma interferograms with a continuous wavelet transform ridge extraction technique: the method," *Appl. Opt.* **40**(35), 6561–6568 (2001).
5. H. Liu, A. Cartwright, and C. Basaran, "Moiré interferogram phase extraction: a ridge detection algorithm for continuous wavelet transforms," *Appl. Opt.* **43**(4), 850–857 (2004).
6. H. Liu, A. Cartwright, and C. Basaran, "Experimental verification of improvement of phase shifting moiré interferometry using wavelet-based image processing," *Opt. Eng.* **43**(5), 1206–1214 (2004).
7. J. Zhong and J. Weng, "Spatial carrier-fringe pattern analysis by means of wavelet transform: wavelet transform profilometry," *Appl. Opt.* **43**(26), 4993–4998 (2004).
8. K. Kadooka, K. Kunoo, N. Uda, K. Ono, and T. Nagayasu, "Strain analysis for moiré interferometry using the two-dimensional continuous wavelet transform," *Exp. Mech.* **43**(1), 45–51 (2003).
9. Z. Wang and H. Ma, "Automatic analysis of photomechanics interferogram using wavelet transform," in *Proc. 2005 SEM Annual Conference and Exposition on Experimental and Applied Mechanics* (2005).
10. B. Telfer and H. Szu, "New wavelet transform normalization to remove frequency bias," *Opt. Eng.* **31**(9), 1830–1834 (1992).



Zhaoyang Wang received his PhD degrees from Tsinghua University in China in 1999 and from the University of Maryland at College Park in 2003. He is currently an assistant professor in the Department of Mechanical Engineering at the Catholic University of America. His research interests include micro- and nanomechanics, optical methods, electronic packaging, computer vision, and image processing.



Huanfeng Ma received his BS degree from Northwestern Polytechnical University in 1993, and his MS degree from Beijing Institute of Technology in 1996, both in electrical engineering and in China. Between 1996 and 1998, he was a lecturer in the Electrical Engineering Department of Beijing Institute of Technology. Mr. Ma is currently a PhD candidate in Electrical and Computer Engineering Department at the University of Maryland, College Park. His research includes image processing, multilingual document analysis and processing, and pattern recognition.